

Observation of a Devil's Staircase in the Novel Spin-Valve System SrCo₆O₁₁

T. Matsuda,¹ S. Partzsch,² T. Tsuyama,^{1,3} E. Schierle,⁴ E. Weschke,⁴ J. Geck,² T. Saito,⁵ S. Ishiwata,¹
Y. Tokura,^{1,6,*} and H. Wadati^{1,3,*}

¹Department of Applied Physics and Quantum-Phase Electronics Center (QPEC), University of Tokyo, Hongo, Tokyo 113-8656, Japan

²Leibniz Institute for Solid State and Materials Research IFW Dresden, Helmholtzstrasse 20, 01069 Dresden, Germany

³Institute for Solid State Physics, University of Tokyo, Kashiwanoha 5-1-5, Chiba 277-8581, Japan

⁴Helmholtz-Zentrum Berlin für Materialien und Energie, Albert-Einstein-Straße 15, 12489 Berlin, Germany

⁵Institute for Chemical Research, Kyoto University, Uji, Kyoto 611-0011, Japan

⁶RIKEN Center for Emergent Matter Science (CEMS), Wako, Saitama 351-0198, Japan

(Received 25 December 2014; published 11 June 2015)

Using resonant soft-x-ray scattering as a function of both temperature and magnetic field, we reveal a large number of almost degenerate magnetic orders in SrCo₆O₁₁. The Ising-like spins in this frustrated material in fact exhibit a so-called magnetic devil's staircase. It is demonstrated how a magnetic field induces transitions between different microscopic spin configurations, which is responsible for the magnetoresistance of SrCo₆O₁₁. This material therefore constitutes a unique combination of a magnetic devil's staircase and spin-valve effects, yielding a novel type of magnetoresistance system.

DOI: 10.1103/PhysRevLett.114.236403

PACS numbers: 71.30.+h, 71.28.+d, 73.61.-r, 79.60.Dp

Combining different materials in artificial nanostructures is a most important approach to create improved or even completely new electronic functionalities for technological applications. A very prominent example of this is the giant magnetoresistance (GMR), which was first realized by multilayers of alternating nonmagnetic and ferromagnetic metals [1,2] and which now is an indispensable part of today's information technology. In these GMR systems the electrical resistance is high for an antiparallel alignment of the magnetization in the neighboring magnetic layers, while it is low for a parallel alignment of those magnetizations. For this reason such systems are also referred to as spin valves.

Large or even colossal magnetoresistance can also occur as an intrinsic effect in bulk materials, due to the interplay of mobile charge carriers and localized spins. Here the doped manganites provide the probably most famous examples [3–7]. A particularly interesting material with intrinsic magnetoresistance is the recently discovered Co oxide SrCo₆O₁₁, the lattice structure of which is believed to realize a GMR multilayer system at the atomic scale [8]. Figure 1(a) shows the normalized out-of-plane resistivity $\rho_c(H)/\rho_c(0)$ of SrCo₆O₁₁ ($H\parallel c$), which is a clear manifestation of magnetoresistance in this material [9]. As shown in Fig. 1(b), SrCo₆O₁₁ exhibits a layered crystal structure consisting of three parts: (i) metallic kagome layers formed by the edge-sharing octahedra, (ii) dimerized octahedra, and (iii) trigonal bipyramids. In the following, the Co sites of the kagome layers, the dimerized octahedra and trigonal bipyramids are referred to as Co(1), Co(2), and Co(3), respectively [cf. Fig. 1(b)]. It was shown earlier that the magnetism of SrCo₆O₁₁ is due to localized Ising-like spins of the Co(3) sites, whereas the charge transport happens in the

subsystems containing Co(1) and Co(2) [9]. The metallic kagome layers are hence linked by magnetic layers containing Co(3) and therefore realize a GMR-multilayer structure at the atomic level. The observed strong Ising type anisotropy along the c axis can be explained by a nonvanishing orbital moment and the resulting spin-orbit coupling of Co(3), as discussed earlier for Ca₃Co₂O₆, which also contains Co sites with trigonal local symmetry [10].

One of the most striking magnetic features of SrCo₆O₁₁ observed so far are plateaus in the magnetization as a

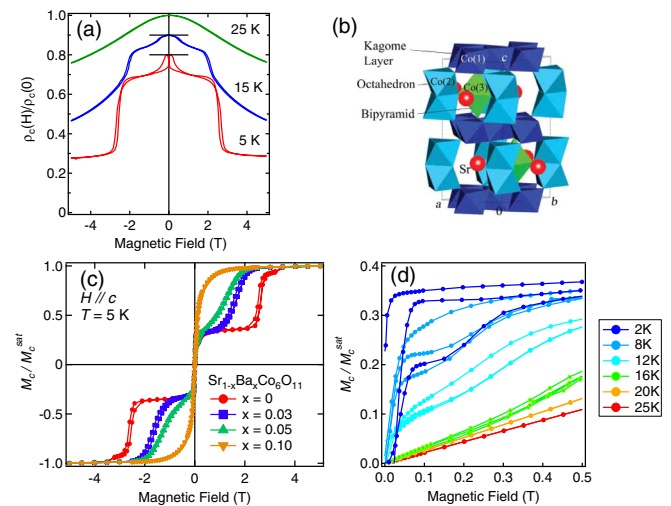


FIG. 1 (color online). (a) Normalized out-of-plane resistivity $\rho_c(H)/\rho_c(0)$ of SrCo₆O₁₁ ($H\parallel c$) taken from Ref. [9]. (b) Crystal structure of SrCo₆O₁₁. (c) Out-of-plane magnetization of Sr_{1-x}Ba_xCo₆O₁₁ as a function of magnetic field ($H\parallel c$) at 5 K. (d) Temperature dependence of out-of-plane magnetization of SrCo₆O₁₁ in low magnetic field region ($H\parallel c$).

function of the applied magnetic field along the c axis [8] as shown in Fig. 1(c). These plateaus correspond to $1/3$ and $3/3$ of the saturated moment [8] and were found to reflect different stackings along c , namely, an up-up-up structure for the $3/3$ phase and an up-up-down configuration for the $1/3$ phase [11]. As in the case of an artificial GMR multilayer, the transition between these magnetic phases are thought to cause the giant magnetoresistance of this compound. Specifically, the magnetic up-up-up structure of the $3/3$ phase [9] leads to less spin scattering and therefore a smaller electrical resistivity than in the up-up-down configuration of the $1/3$ phase [9].

In this Letter, we present a high-resolution resonant soft-x-ray scattering (RSXS) study of $\text{SrCo}_6\text{O}_{11}$ bulk single crystals as a function of temperature (T) and applied magnetic field (H). We discover various metastable magnetic orders in low magnetic fields that escaped detection in earlier experiments. The occurrence of all these metastable phases can be interpreted in terms of strong frustration in a strongly anisotropic magnetic system, which results in a large variety of almost degenerate magnetic structures [12–20]. In fact, our results imply that $\text{SrCo}_6\text{O}_{11}$ is the realization of a magnetic devil's staircase in a $3d$ -electron system. Our central result, therefore, is that magnetic frustration is a fundamental ingredient for the functionality of $\text{SrCo}_6\text{O}_{11}$, which realizes a novel and sensitive GMR system at the atomic level in a single phase material. In addition, the high degree of frustration intrinsically causes a strong sensitivity of the system to external modifications, which consequently opens the possibility of tailoring functionality as demonstrated in this study by Ba substitution at the Sr site.

Pure and Ba-substituted $\text{SrCo}_6\text{O}_{11}$ bulk single crystals were synthesized by the high-pressure technique [8]. The typical sample size was $\approx 0.20 \times 0.20 \times 0.05 \text{ mm}^3$. The out-of-plane magnetization of pure and Ba-substituted $\text{SrCo}_6\text{O}_{11}$ are shown in Figs. 1(c) and 1(d). RSXS is a powerful tool to reveal ordered structures in solids such as magnetic, charge, and orbital ordering [21–26]. Here we employed the strongly enhanced magnetic sensitivity of RSXS at the $\text{Co } 2p_{3/2}$ edge (780 eV) in order to investigate the subtle magnetic phase transitions in our small-volume samples depending on temperature and external magnetic fields. The present study is one of the very first RSXS experiments performed under magnetic fields of several Tesla. The experiments were carried out at the high-field diffractometer operated at the UE46-PGM1 beam line of BESSY-II, Germany. Figure 2(a) shows the scattering geometry used for the present experiments. Temperatures down to 4 K could be reached using a continuous helium-flow cryostat. X-ray polarization was linear (σ and π). Applied magnetic field was up to 4 T.

Figure 2(b) shows the diffraction peaks of $\text{SrCo}_6\text{O}_{11}$ at zero field for various temperatures. Quite surprisingly and very uncommon for RSXS experiments, a large number of superlattice reflections at $L = n/6$ with $n = 4, 5, 6, 7, 8,$

and 9 is observed. The small and temperature independent peak at $L = 1.37$ is assigned to some impurity in the sample because it does not show temperature dependence. $L = 1$ commensurate (CM) peak and two incommensurate (ICM) peaks around $L = 0.8, 1.2$ appear at 20 K (T_{c1}). These ICM peaks move to $L = 5/6$ and $7/6$, respectively, as the temperature is decreased, and finally are locked at these values at 12 K (T_{c2}), respectively. At T_{c2} , there appear $L = 6/5$ and $8/7$ shoulders of the $L = 7/6$, and, simultaneously, $L = 2/3, 4/3,$ and $3/2$ peaks.

Intensities of all the magnetic peaks were independent of the polarizations σ and π , as shown in Fig. 2(c) for the case of $L = 6/5$. For spins along the c direction, the magnetic scattering factor can be expressed as

$$f_{\text{mag}} = \begin{matrix} \sigma & \pi \\ \sigma' \begin{pmatrix} 0 & m_c \sin \theta \\ m_c \sin \theta & 0 \end{pmatrix}, \end{matrix}$$

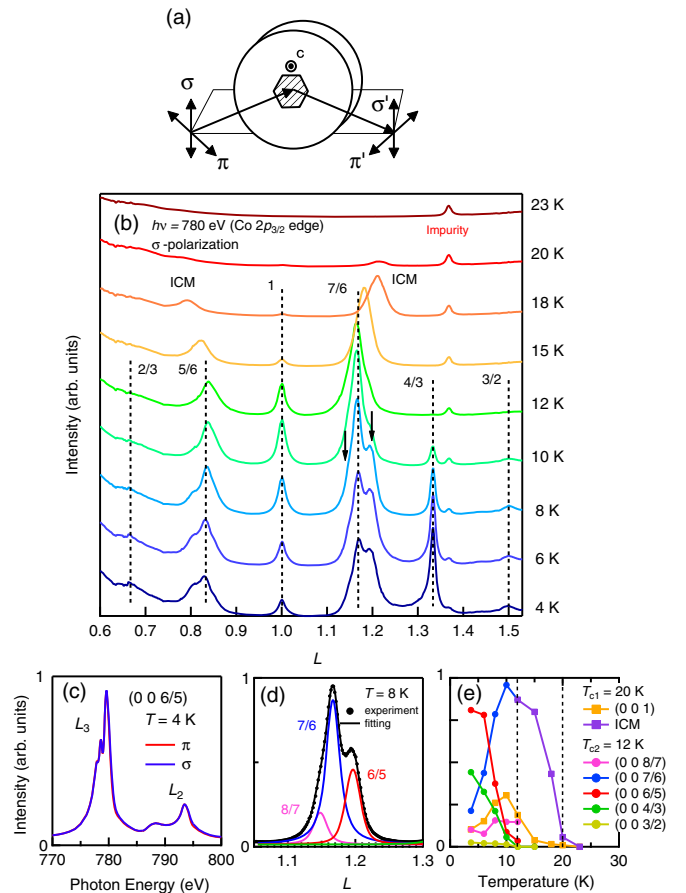


FIG. 2 (color online). (a) Experimental geometry for RSXS measurements. The arrows indicate the directions of polarizations of x rays. (b) Magnetic peak profile of $\text{SrCo}_6\text{O}_{11}$ at various temperatures at zero magnetic field. (c) Photon-energy dependence of intensity of the $L = 6/5$ reflection for σ and π polarizations. (d) Magnetic peak fitting of $\text{SrCo}_6\text{O}_{11}$ around $L = 7/6$. (e) Temperature dependence of the integrated intensity of each magnetic peak.

where m_c is the component of the spins along the c axis and θ is the scattering angle [27,28]. In this case, pure σ - π' and π - σ' channels have the same intensity, which agrees very well with our experimental results and verifies the interpretation in terms of c -axis magnetic scattering.

The emergence of the magnetic $L = 2/3$ and $4/3$ peaks agrees well with the powder neutron diffraction measurement at 2 T [11]. In order to assign the shoulder peaks around $L = 7/6$, the data were fitted by three components of $L = 7/6$, $8/7$, and $6/5$ as shown in Fig. 2(d). These results therefore directly reveal that a large number of magnetic phases coexist in zero magnetic field and, in particular, that the $\uparrow\uparrow\downarrow$ configuration is realized even at zero magnetic field. We observed the magnetic peaks of $L = n/6$ with $n = 4, 5, 6, 7, 8$, and 9 . However, the temperature dependence varies for different n and the peaks with $n = 5$ and 7 show the shift from ICM to CM peak position and the others do not. This indicates that all the different peaks cannot be due to one magnetic modulation with $L = 1/6$ but belong to different magnetic stacking sequences. This is clearly seen in the different temperature-dependent behaviors of these magnetic peaks shown in Fig. 2(e), and is also reflected in the observed field dependent behavior.

All the magnetic peaks are rather broad and the full widths at half maximum (FWHM) $\Delta L \sim (0.02-0.03)$ r.l.u., suggesting that the correlation length along the c axis is only a few tens of unit cells. All the spins are Ising type in this material, so the magnetic state is not the coexistence on the same sites, but domains with each magnetic ordering are expected to be spatially separated. Future submicron spatially resolved RSXS measurements will further reveal the nature of this coexistent state.

The geometry of the x-ray beam and the superconducting magnet for the field-dependent experiment is shown in Fig. 3(a). Figure 3(b) shows the magnetic peaks at 12 K around $L = 4/5$. The denoted values of the magnetic field are the c -axis component because the ab component is irrelevant to the magnetic structures due to the strong Ising-like anisotropy [9,11]. The $L = 5/6$ peak has strong intensity around $H = 0$ T, while the $4/5$ peak is stabilized

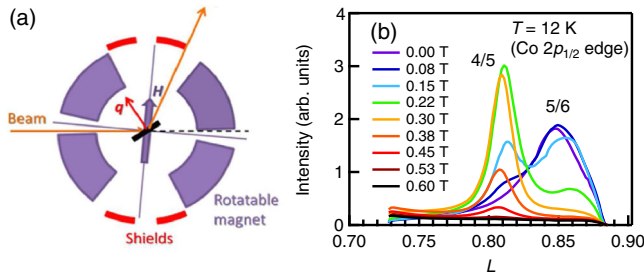


FIG. 3 (color online). Geometry for RSXS under magnetic field (a), and magnetic peaks observed under various field (b). The denoted values of the magnetic field are the c -axis component.

around $H = 0.2$ T, indicating that the magnetic peaks with different L behave differently under magnetic fields.

In this way, we have been able to explore the entire H - T diagram of this complex magnetic system as shown in Fig. 4. Here, $\langle n \rangle$ represents the magnetic periodicities. Since the $\text{SrCo}_6\text{O}_{11}$ unit cell contains two equivalent $\text{Co}(3)$ Bragg planes along c , (002) is the first allowed structural reflections and (001) corresponds to a simple $\uparrow\downarrow\uparrow\downarrow$ antiferromagnetic order. Therefore, $\langle 2 \rangle$ corresponds to $L = 1$, $\langle 3 \rangle$ to $L = 4/3$, $\langle 4 \rangle$ to $L = 3/2$, $\langle 5 \rangle$ to $L = 4/5$, and $\langle 12 \rangle$ to $L = 5/6$. The phase boundary between $\uparrow\uparrow\uparrow$ (saturated) and $\uparrow\uparrow\downarrow$ ($\langle 3 \rangle$) states was determined by magnetization measurements, and the other boundaries were determined by the present RSXS results. The phase diagram demonstrates that various magnetic orderings with different periodicities are formed in the low temperature and low field region. Obviously, the energies of these magnetic structures are quite close, and the corresponding energy differences sensitively depend on temperature and magnetic fields. A similar behavior has been observed in CeSb , which also has various magnetic orderings depending on temperature and field [12–14]. This phenomenon is called “the devil’s staircase,” where, in principle, an infinite number of commensurate superstructures can be realized by tuning an external parameter. As these corresponding eigenstates (magnetic orderings in this case) have similar

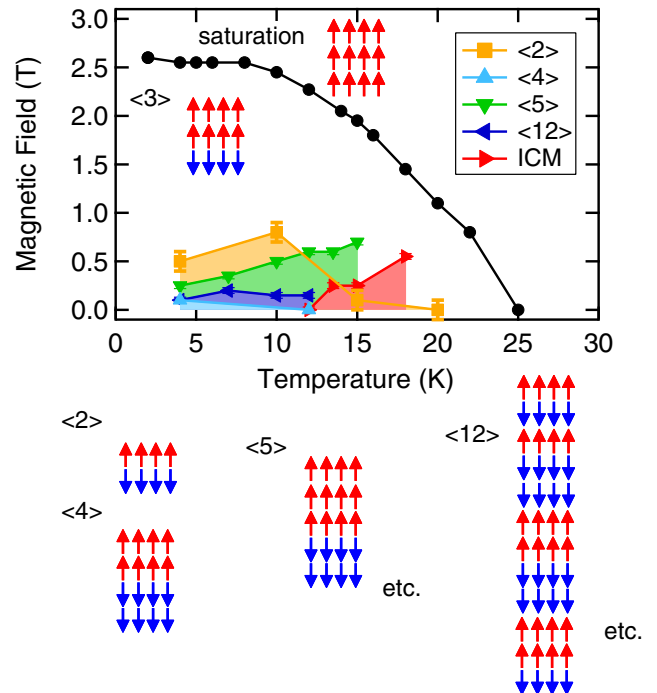


FIG. 4 (color online). Magnetic phase diagram of $\text{SrCo}_6\text{O}_{11}$ determined by RSXS measurements. The phase boundary between $\uparrow\uparrow\uparrow$ and $\uparrow\uparrow\downarrow$ states was determined by magnetization measurements. The colored areas represent the regions where the corresponding orderings exist. $\langle 3 \rangle$ exists in the whole region of 0–2.6 T at 4 K.

energies, they can be switched from one to another by small perturbation. In this case of magnetic ordering, the mechanism is described by the axial next-nearest-neighbor Ising (ANNNI) model [12–20]. The ANNNI model describes competing interactions between nearest (J_1) and next-nearest (J_2) Ising spins, which yields various magnetic orderings with close energies in the phase diagram of temperature and J_2/J_1 .

In $\text{SrCo}_6\text{O}_{11}$ the situation is very similar in that (i) $\text{Co}(3)$ has a strong Ising anisotropy and (ii) our RSXS results reveal a coexistence of various essentially degenerate magnetic phases. We therefore conclude that $\text{SrCo}_6\text{O}_{11}$ indeed exhibits a devil's staircase scenario, i.e., a coexistence of a large number of magnetic periodicities with almost the same energies. Such coexistence is destroyed by the application of an external magnetic field, selecting only those phases that are energetically favorable now, leading to the magnetization plateaus observed in macroscopic measurements. Therefore, $\text{SrCo}_6\text{O}_{11}$ is considered as the example of the devil's staircase in a $3d$ -electron spin system.

However, in order to explain ordered structures with long periodicities, one needs magnetic interactions that go well beyond the nearest neighbors. A plausible explanation can be provided by the Ruderman-Kittel-Kasuya-Yosida (RKKY) interaction via the metallic planes. $\text{SrCo}_6\text{O}_{11}$ has strong coupling between conduction electrons and localized spins, where RKKY interactions play the most important role. Consequently, the very complex behavior of the magnetically highly frustrated $\text{SrCo}_6\text{O}_{11}$ is far beyond the description of the simple ANNNI model. It may be better described by a more complex model with both localized spins and conduction electrons.

Interestingly, the observed very complex microscopic magnetic behavior seems to be also reflected in the macroscopic material properties: The out-of-plane magnetization at low temperatures in low magnetic fields in Fig. 1(d) shows hysteresis and additional plateaus around $1/5$. These plateaus are caused by the phases of $L = 4/5$, which have a smaller magnetization than the $1/3$ phase. However, finally, the strongest ferrimagnetic phase ($L = 4/3$) is the only remaining phase in higher magnetic fields, which creates the $1/3$ magnetization plateau. This field- and temperature-dependent magnetization is closely linked to the measured normalized out-of-plane resistivity $\rho_c(H)/\rho_c(0)$, which is characterized by several plateaus and hysteretic behavior in the low-field region as shown in Fig. 1(a). These macroscopic properties can be easily understood on the basis of the observed magnetic phase diagram: The magnetic phases in the low-field region are connected with anomalies in magnetization and resistivity since the magnetic field is able to select and stabilize single phases out of this “nearly degenerate ground state.” Hence, the basic mechanism behind functionality of the novel spin-valve system $\text{SrCo}_6\text{O}_{11}$ is a very high degree of magnetic

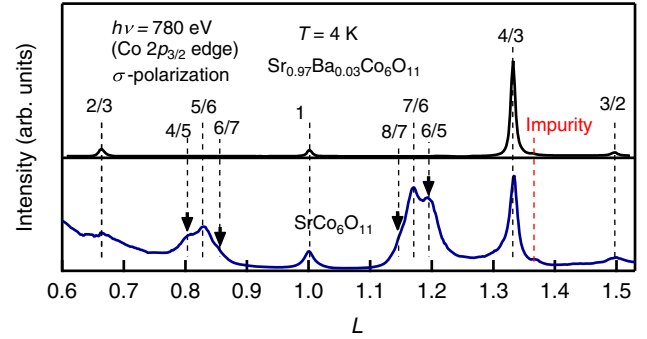


FIG. 5 (color online). Magnetic peaks at zero field of $\text{SrCo}_6\text{O}_{11}$ and $\text{Sr}_{0.97}\text{Ba}_{0.03}\text{Co}_6\text{O}_{11}$ at 4 K.

frustration leading to a complex magnetic phase mixture whose delicate balance can be easily modified even by small magnetic fields.

Besides the related magnetoresistive functionality, frustrated magnets are also very sensitive to chemical doping. In contrast to robust systems, which require substantial doping to alter material properties, here a fine-tuning of material properties should be possible by very low doping, in this way preventing unwanted side effects. This is demonstrated in the present study by Ba substitution of Sr of only a few percent as shown in Fig. 5. In $\text{Sr}_{0.97}\text{Ba}_{0.03}\text{Co}_6\text{O}_{11}$ one cannot see any magnetic peaks around $L = 5/6$ or $7/6$, demonstrating that small Ba substitution of only 3% destroys almost the degenerate ground states, and, consequently, shifts the $1/3 \rightarrow 3/3$ functional step to lower magnetic fields. Stronger substitution of 10% shifts this step to 0 T, i.e., the system has a ferromagnetic ground state as shown in Fig. 1(c).

In summary, we have investigated the magnetic structures of $\text{SrCo}_6\text{O}_{11}$ bulk single crystals. We observed the devil's staircase behavior in a $3d$ system where coupling is mediated by RKKY interaction. This is a consequence of highly frustrated magnetic systems. The ground state, where there is a coexistence of various magnetic periodicities with almost the same energies, is very susceptible to magnetic fields and, finally, is the responsible mechanism behind the observed macroscopic functionality. In connection with the layered structure and Ising-like anisotropy, this generates a spin-valve functionality in a single phase material, which usually requires complex heterostructures. Furthermore, having frustration as the fundamental mechanism, this system can be easily tunable, raising the hope for engineered system properties, which has been demonstrated here by studying the behavior depending on very small amount of Ba doping.

This work was supported by the Japan Society for the Promotion of Science (JSPS) through the “Funding Program for World-Leading Innovative R&D on Science and Technology (FIRST Program)” initiated by the Council for Science and Technology Policy (CSTP), and in part by

JSPS Grant-in-Aid for Scientific Research(S) No. 24224009. This work was also partially supported by the Ministry of Education, Culture, Sports, Science and Technology of Japan (X-ray Free Electron Laser Priority Strategy Program) and by a research grant from The Murata Science Foundation. S. P. and J. G. thank the DFG for the support through the Emmy Noether Program (Grant No. GE 1647/2-1).

*wadati@issp.u-tokyo.ac.jp;

<http://www.geocities.jp/qxbqd097/index2.htm>

- [1] M. N. Baibich, J. M. Broto, A. Fert, F. Nguyen Van Dau, F. Petroff, P. Etienne, G. Creuzet, A. Friederich, and J. Chazelas, *Phys. Rev. Lett.* **61**, 2472 (1988).
- [2] G. Binasch, P. Grünberg, F. Saurenbach, and W. Zinn, *Phys. Rev. B* **39**, 4828 (1989).
- [3] A. P. Ramirez, *J. Phys. Condens. Matter* **9**, 8171 (1997).
- [4] C. N. R. Rao, A. Arulraj, A. K. Cheetham, and B. Raveau, *J. Phys. Condens. Matter* **12**, R83 (2000).
- [5] W. Prellier, P. Lecoeur, and B. Mercey, *J. Phys. Condens. Matter* **13**, R915 (2001).
- [6] A. M. Haghiri-Gosnet and J. P. Renard, *J. Phys. D* **36**, R127 (2003).
- [7] Y. Tokura, *Rep. Prog. Phys.* **69**, 797 (2006).
- [8] S. Ishiwata, D. Wang, T. Saito, and M. Takano, *Chem. Mater.* **17**, 2789 (2005).
- [9] S. Ishiwata, I. Terasaki, F. Ishii, N. Nagaosa, H. Mukuda, Y. Kitaoka, T. Saito, and M. Takano, *Phys. Rev. Lett.* **98**, 217201 (2007).
- [10] H. Wu, M. W. Haverkort, Z. Hu, D. I. Khomskii, and L. H. Tjeng, *Phys. Rev. Lett.* **95**, 186401 (2005).
- [11] T. Saito, A. Williams, J. P. Attfield, T. Wuernisha, T. Kamiyama, S. Ishiwata, Y. Takeda, Y. Shimakawa, and M. Takano, *J. Magn. Magn. Mater.* **310**, 1584 (2007).
- [12] P. Bak, *Rep. Prog. Phys.* **45**, 587 (1982).
- [13] J. R.-Mignod, P. Burlet, J. Villain, H. Bartholin, W. Tcheng-Si, D. Florence, and O. Vogt, *Phys. Rev. B* **16**, 440 (1977).
- [14] J. R.-Mignod, J. M. Effantin, P. Burlet, T. Chattopadhyay, L. P. Regnault, H. Bartholin, C. Vettier, O. Vogt, D. Ravot, and J. C. Achard, *J. Magn. Magn. Mater.* **52**, 111 (1985).
- [15] M. Takigawa, M. Horvatic, T. Waki, S. Kramer, C. Berthier, F. Levy-Bertrand, I. Sheikin, H. Kageyama, Y. Ueda, and F. Mila, *Phys. Rev. Lett.* **110**, 067210 (2013).
- [16] K. Ohwada, Y. Fujii, N. Takesue, M. Isobe, Y. Ueda, H. Nakao, Y. Wakabayashi, Y. Murakami, K. Ito, Y. Amemiya, H. Fujihisa, K. Aoki, T. Shobu, Y. Noda, and N. Ikeda, *Phys. Rev. Lett.* **87**, 086402 (2001).
- [17] J. von Boehm and P. Bak, *Phys. Rev. Lett.* **42**, 122 (1979).
- [18] P. Bak and J. von Boehm, *Phys. Rev. B* **21**, 5297 (1980).
- [19] W. Selke and P. M. Duxbury, *Z. Phys. B* **57**, 49 (1984).
- [20] K. Nakanishi, *J. Phys. Soc. Jpn.* **58**, 1296 (1989).
- [21] J. Fink, E. Schierle, E. Weschke, and J. Geck, *Rep. Prog. Phys.* **76**, 056502 (2013).
- [22] H. Wadati, J. Okamoto, M. Garganourakis, V. Scagnoli, U. Staub, Y. Yamasaki, H. Nakao, Y. Murakami, M. Mochizuki, M. Nakamura, M. Kawasaki, and Y. Tokura, *Phys. Rev. Lett.* **108**, 047203 (2012).
- [23] S. Partzsch, S. B. Wilkins, J. P. Hill, E. Schierle, E. Weschke, D. Souptel, B. Büchner, and J. Geck, *Phys. Rev. Lett.* **107**, 057201 (2011).
- [24] S. Y. Zhou, Y. Zhu, M. C. Langner, Y.-D. Chuang, P. Yu, W. L. Yang, A. G. Cruz Gonzalez, N. Tahir, M. Rini, Y.-H. Chu, R. Ramesh, D.-H. Lee, Y. Tomioka, Y. Tokura, Z. Hussain, and R. W. Schoenlein, *Phys. Rev. Lett.* **106**, 186404 (2011).
- [25] T. A. W. Beale, S. B. Wilkins, R. D. Johnson, S. R. Bland, Y. Joly, T. R. Forrest, D. F. McMorrow, F. Yakhou, D. Prabhakaran, A. T. Boothroyd, and P. D. Hatton, *Phys. Rev. Lett.* **105**, 087203 (2010).
- [26] S. Smadici, J. C. T. Lee, S. Wang, P. Abbamonte, G. Logvenov, A. Gozar, C. Deville Cavellin, and I. Bozovic, *Phys. Rev. Lett.* **102**, 107004 (2009).
- [27] J. P. Hannon, G. T. Trammell, M. Blume, and D. Gibbs, *Phys. Rev. Lett.* **61**, 1245 (1988).
- [28] J. P. Hill and D. F. McMorrow, *Acta Crystallogr. Sect. A* **52**, 236 (1996).